#1
1557 Section Copy

NACA TN No. 1600

NATIONAL ADVISORY COMMITTEE FOR AERONAUTICS

TECHNICAL NOTE

No. 1600

CHARACTERISTICS OF THIN TRIANGULAR WINGS WITH TRIANGULAR-TIP CONTROL SURFACES AT SUPERSONIC SPEEDS WITH MACH LINES BEHIND THE LEADING EDGE

By Warren A. Tucker

Langley Memorial Aeronautical Laboratory
Langley Field, Va.

Washington
May 1948

NATIONAL ADVISORY COMMITTEE FOR AERONAUTICS

TECHNICAL NOTE NO. 1600

CHARACTERISTICS OF THIN TRIANGULAR WINGS WITH TRIANGULAR-TIP CONTROL SURFACES AT SUPERSONIC SPEEDS WITH MACH LINES BEHIND THE LEADING EDGE

By Warren A. Tucker

SUMMARY

A theoretical analysis, based on the linearized equation for supersonic flow, was made of the characteristics of triangular-tip control surfaces on thin triangular wings. By restricting the analysis to the case for which the Mach lines from the wing apex lie behind the leading edge, a simplified treatment was made possible in that the results of previous work on the lift of triangular wings could be used to derive simple expressions for the lift effectiveness, pitching moment, rolling-moment effectiveness, and hinge moment due to control deflection. An expression was also obtained for the hinge moment due to angle of attack. Comparisons were made with the results for the two-dimensional case.

The ratio of lift effectiveness to the hinge moment which resulted from control deflection was equal to the corresponding two-dimensional ratio for the same ratio of flap area to wing area.

Again for equal ratios of flap area to wing area and for a flap chord one-half the wing chord, the rate of roll per hinge-moment coefficient due to control deflection was twice as large for the present configuration as for the two-dimensional case. This difference was directly a result of the difference in damping coefficients between the two cases.

The values of hinge-moment coefficient due to angle of attack were found to be high when compared with either the hinge-moment coefficient due to control deflection or with the two-dimensional hinge-moment coefficient due to angle of attack. The appreciable balancing effect thus indicated would materially reduce the stick force in a steady roll and would also have to be taken into account in the determination of the stick-free longitudinal stability if the present arrangement were used as a horizontal tail.

INTRODUCTION

There is considerable interest in the use of wings having triangular plan forms for flight at supersonic speeds. Much work has been done on the lift and drag characteristics of such wings (references 1 to 5). Investigation of the lift and hinge-moment characteristics of control surfaces which might be used on triangular wings was considered desirable. Several such control surfaces have been suggested; the present paper treats control surfaces which are located at the tips of the wing and which have plan forms geometrically similar to the plan form of the wing.

The present analysis is restricted to the case in which the Mach lines from the apex of the wing lie behind the leading edge. Because of this restriction, the results of reference 2 could be used to obtain simple expressions for the lift effectiveness, rolling-moment effectiveness, pitching moment, and hinge moment due to control deflection. An expression was also obtained for the hinge moment due to angle of attack.

Because the analysis of reference 2, which forms the basis for the present paper, was made by use of the linearized equations of motion, the present results are valid only within the usual limits of the linearized theory. Also, the effects of viscosity have been neglected. In this regard, some preliminary experimental results on a flapped airfoil have indicated that a fully developed boundary layer may reduce the effective angle of flap deflection.

SYMBOLS

b	maximum wing span
b_f	trailing-edge span of one flap
b_f'	hinge-line span of one flap
c	wing root chord
c_l	wing local chord
$\bar{c}$	wing mean aerodynamic chord $\left(\frac{2}{S}\int_0^{b/2} c_l^2\, dy = \frac{2}{3}c\right)$
c_f	maximum flap chord in free-stream direction

$\bar{c}_f$ flap root-mean-square chord perpendicular to hinge line $\left(\frac{2}{\sqrt{3}} c_f \sin \epsilon\right)$

C_L lift coefficient $\left(\frac{\text{Lift}}{qS}\right)$

C_m pitching-moment coefficient about wing aerodynamic center $\left(\frac{\text{Pitching moment}}{qS\bar{c}}\right)$

C_l rolling-moment coefficient $\left(\frac{\text{Rolling moment}}{qSb}\right)$

C_h hinge-moment coefficient $\left(\frac{H}{qb_f' \bar{c}_f^2}\right)$

C_p pressure coefficient $\left(\frac{p - p_o}{q}\right)$

$$F_1 \equiv \frac{c^3}{3} - c^2(c - c_f)$$

$$F_2 \equiv \frac{c^3}{3}$$

$$F_3 \equiv \frac{4}{3}(c - c_f)^3$$

$$G_1 \equiv -\frac{2}{3}\left(\frac{c}{c_f}\right)^3 + \left(\frac{c}{c_f}\right)^2$$

$$G_2 \equiv \frac{1}{3}\left(\frac{c}{c_f}\right)^3$$

$$G_3 \equiv \frac{4}{3}\left(\frac{c}{c_f} - 1\right)^3$$

H hinge moment of one flap

M free-stream Mach number

$$n \equiv \frac{\tan \mu}{\tan \epsilon}$$

p pressure on one surface; rolling velocity

p_o free-stream pressure

P lifting pressure on flap

q free-stream dynamic pressure $\left(\frac{\rho V^2}{2}\right)$

R perpendicular distance from hinge line of one flap to opposite leading edge (see fig. 6)

S wing area

S_f area of two flaps

$t \equiv \frac{\tan \zeta}{\tan \epsilon}$

$t_o = 1 - 2\left(\frac{c_f}{c}\right)$

V free-stream velocity

w disturbance velocity in z-direction (αV)

x,y Cartesian coordinates parallel and normal, respectively, to free-stream direction with origin at wing apex

y_f distance from wing center line to flap center line

α angle of attack

α_δ lift effectiveness $\left(C_{L_\delta}/C_{L_\alpha}\right)$

$\beta \equiv \sqrt{M^2 - 1}$

δ angle of flap deflection about hinge line

ϵ wing-semiapex angle

$\zeta = \tan^{-1} \frac{y}{x}$

μ Mach angle $\left(\tan^{-1} \frac{1}{\beta}\right)$

ρ free-stream density

$\sigma = \sqrt{\frac{n^2 - t^2}{1 - t^2}}$

ϕ_x disturbance velocity in x-direction

Subscripts:

α partial derivative of coefficient with respect to α $\left(\text{example: } C_{L_\alpha} \equiv \frac{\partial C_L}{\partial \alpha}\right)$

δ partial derivative of coefficient with respect to δ (except when used in α_δ)

C_L partial derivative of coefficient with respect to C_L

∞ two-dimensional case

All angles are in radians unless otherwise specified.

ANALYSIS

Lift Effectiveness

The control-surface configuration under investigation is shown in figure 1. There is no change in pressure over the main surface of the wing when the flaps are deflected as long as the Mach lines lie behind the leading edge. The lift produced by a given flap deflection can therefore be found by regarding each flap as an isolated triangular wing. Had the restriction not been imposed that the Mach lines lie behind the leading edge, then not only would consideration of the effect of the flap on the wing have been necessary, but, in addition, the upwash about the outside edge of the flap would have had to be taken into account. With the present restriction, the center of pressure on the deflected flap is always at the center of flap area, which greatly simplifies the analysis.

For a small flap deflection δ about the hinge line, the corresponding angle of attack of the flap to the free stream can easily be shown to be $\delta \sin \epsilon$. From reference 2, the lift coefficient (based on total wing area S) caused by a flap deflection δ may then be shown to be

$$C_L = \frac{4\delta \sin \epsilon}{\beta} \frac{S_f}{S} \tag{1}$$

From the geometry of the configuration,

$$\frac{S_f}{S} = 2\left(\frac{c_f}{c}\right)^2$$

therefore,

$$C_L = \frac{8\delta \sin \epsilon}{\beta} \left(\frac{c_f}{c}\right)^2$$

and

$$C_{L_\delta} = \frac{8 \sin \epsilon}{\beta} \left(\frac{c_f}{c}\right)^2 \tag{2}$$

It is common practice to define the lift effectiveness of a control surface as α_δ, which may be considered as the ratio of the lift coefficient produced by a unit flap deflection to the lift coefficient produced by a unit angle of attack of the entire wing. From reference 2, the lift coefficient produced by a unit angle of attack is

$$C_{L_\alpha} = \frac{4}{\beta} \tag{3}$$

The lift effectiveness is therefore

$$\alpha_\delta = \frac{C_{L_\delta}}{C_{L_\alpha}} = 2 \sin \epsilon \left(\frac{c_f}{c}\right)^2 \tag{4}$$

Values of α_δ are given in figure 2. Note that at $\frac{c_f}{c} = 0.5$ the inboard ends of the trailing edges of the two flaps meet at the center line of the wing; therefore, this is the largest flap chord

ratio that can be used with this scheme. At $\epsilon = 90^\circ$ the wing reduces to a straight line; consequently, this value of ϵ represents a limiting case rather than a physically possible configuration.

At this point the corresponding lift parameters may be conveniently given for a two-dimensional wing with a constant-chord flap. For the two-dimensional case, the following equations from reference 6 may be given

$$C_{L_{\delta_\infty}} = \frac{4}{\beta} \frac{c_f}{c} \tag{5}$$

and

$$C_{L_{\alpha_\infty}} = \frac{4}{\beta} \tag{6}$$

therefore,

$$\alpha_{\delta_\infty} = \frac{C_{L_{\delta_\infty}}}{C_{L_{\alpha_\infty}}} = \left(\frac{c_f}{c}\right)_\infty \tag{7}$$

A direct comparison of α_δ to α_{δ_∞} is not particularly enlightening. In a later section of the paper ("Discussion and Concluding Remarks"), a more definitive comparison, involving hinge moments, is made.

Pitching Moment

When the flap is deflected, the angle of attack being held constant, the resultant lift on the flap usually gives rise to a pitching moment. This effect is of importance in stability work, and its magnitude may be evaluated if the fact is remembered that the center of pressure on the deflected flap is at two-thirds of the flap chord from the flap apex.

The pitching moment is found about the aerodynamic center of the main wing, which is at two-thirds of the wing chord from the wing apex. The pitching-moment coefficient is based on total wing area and wing mean aerodynamic chord, which can be shown to equal $\frac{2}{3}c$.

Then,

$$C_m = -\frac{C_L qS\left(\frac{c}{3} - \frac{c_f}{3}\right)}{qS\frac{2c}{3}}$$

$$= -\frac{C_L}{2}\left(1 - \frac{c_f}{c}\right)$$

and

$$C_{m_{C_L}} = -\frac{1}{2}\left(1 - \frac{c_f}{c}\right) \tag{8}$$

Values of $-C_{m_{C_L}}$ are shown in figure 3.

Again, comparison of this pitching-moment coefficient with that for the two-dimensional case is of interest. When reference 6 is used, the pitching-moment coefficient about the wing aerodynamic center (which now is at the midchord) resulting from a unit lift coefficient due to flap deflection can be shown to be

$$C_{m_{C_{L_\infty}}} = -\frac{1}{2}\left(1 - \frac{c_f}{c}\right) \tag{9}$$

so that for equal flap chord ratios

$$\frac{C_{m_{C_L}}}{C_{m_{C_{L_\infty}}}} = 1 \tag{10}$$

From figure 3 the value of $-C_{m_{C_L}}$ is the smallest for the largest flap size. Whether a large or small value of $C_{m_{C_L}}$ is desirable depends upon the type of control surface (elevator or aileron).

Rolling-Moment Effectiveness

If the two flaps are deflected equal amounts in opposite directions, a rolling moment rather than a lift force is produced. An expression is now found for the rolling-moment coefficient resulting from unit deflections of the flaps in opposite directions. If the rolling-moment coefficient is based on total wing area and wing span, the rolling-moment coefficient produced by opposite unit deflections of the flaps is given by

$$C_{l_\delta} = \frac{C_{L_\delta} q S y_f}{qSb} = C_{L_\delta} \frac{y_f}{b} \tag{11}$$

Now,

$$y_f = \frac{b}{2} - \frac{b_f}{2}$$

therefore,

$$\frac{y_f}{b} = \frac{1}{2}\left(1 - \frac{b_f}{b}\right) = \frac{1}{2}\left(1 - \frac{c_f}{c}\right)$$

and by substitution of equation (2), equation (11) becomes

$$C_{l_\delta} = \frac{4 \sin \epsilon}{\beta} \left(\frac{c_f}{c}\right)^2 \left(1 - \frac{c_f}{c}\right) \tag{12}$$

Values of $C_{l_\delta}\beta$ are given in figure 4.

The rolling-moment coefficient for the two-dimensional case can be shown to be

$$C_{l_{\delta_\infty}} = \frac{1}{\beta}\left(\frac{c_f}{c}\right)_\infty \tag{13}$$

The rolling-moment effectiveness is often used to determine the rate of roll as expressed by the wing-tip helix angle $pb/2V$. In

order to obtain the value of $pb/2V$ for a unit aileron deflection, C_{l_δ} is divided by the damping coefficient of the wing, defined as

$$C_{l_p} \equiv \frac{\partial C_l}{\partial \frac{pb}{2V}} \tag{14}$$

For the triangular wing with the Mach lines behind the leading edge, the damping in roll has been found in reference 7 to be

$$C_{l_p} = \frac{1}{3\beta} \tag{15}$$

and for the two-dimensional wing

$$C_{l_{p_\infty}} = \frac{2}{3\beta} \tag{16}$$

so that

$$\frac{pb/2V}{\delta} = 12 \sin \epsilon \left(\frac{c_f}{c}\right)^2 \left(1 - \frac{c_f}{c}\right) \tag{17}$$

and

$$\left(\frac{pb/2V}{\delta}\right)_\infty = \frac{3}{2}\left(\frac{c_f}{c}\right)_\infty \tag{18}$$

Hinge Moment Due to Control Deflection

Not only the forces and moments produced by the flaps, but also the forces required to move the flaps, are of concern to the aircraft designer. The hinge moment resulting from flap deflection can be found in much the same fashion as the pitching moment resulting from flap deflection, if the center of pressure on the deflected flap is remembered to be at the center of area of the flap. If the usual convention is followed in which the hinge-moment coefficient is based

on the maximum flap span along the hinge line and on the square of the flap root-mean-square chord measured perpendicular to the hinge line, the hinge-moment coefficient produced by a unit flap deflection can be found.

The flap span along the hinge is seen to be

$$b_f' = c_f \sec \epsilon \tag{19}$$

The square of the flap root-mean-square chord perpendicular to the hinge line can most conveniently be found by taking twice the area moment of one flap about its hinge line and dividing by the hinge-line span of one flap and is found to be

$$\bar{c}_f^2 = \frac{4}{3} c_f^2 \sin^2 \epsilon \tag{20}$$

Using a lift coefficient based on the area of one flap rather than on wing area is also convenient and, therefore, from equation (1)

$$C_{L_\delta} = \frac{4 \sin \epsilon}{\beta}$$

The hinge-moment coefficient for a unit flap deflection can now be written

$$C_{h_\delta} = -\frac{\frac{4 \sin \epsilon}{\beta} \frac{b_f c_f}{2} \frac{2}{3} c_f q \sin \epsilon}{q c_f b_f \sec \epsilon \frac{4}{3} c_f^2 \sin^2 \epsilon} = -\frac{b_f \cos \epsilon}{c_f \beta}$$

but

$$\frac{b_f}{c_f} = 2 \tan \epsilon$$

therefore,

$$C_{h_\delta} = -\frac{2}{\beta} \sin \epsilon \tag{21}$$

Values of $-C_{h_\delta}\beta/2$ are presented in figure 5. The value of C_{h_δ} for the two-dimensional case (see reference 6) is

$$C_{h_{\delta_\infty}} = -\frac{2}{\beta} \tag{22}$$

therefore,

$$\frac{C_{h_\delta}}{C_{h_{\delta_\infty}}} = \sin \epsilon \tag{23}$$

Since this ratio is merely $-C_{h_\delta}\beta/2$, figure 5 also represents a plot of equation (23). For the present configuration C_{h_δ} is always less than for the two-dimensional case, and the value of C_{h_δ} is independent of flap size.

Hinge Moment Due to Angle of Attack

In the analysis thus far, obtaining simple expressions for the various aerodynamic characteristics has been possible by virtue of the fact that the deflected flap could be regarded as an isolated triangular wing, the lift of which could be expressed very simply without the need of any pressure integration over the flap surface. This simple concept cannot be used to determine the flap hinge moment resulting from an angle of attack of the entire wing. Instead, an integration of the elementary hinge moment over the surface of the flap must be performed.

Because of the conical flow field produced by the triangular wing at an angle of attack, the pressure is constant along any straight line emanating from the wing apex, the value of the constant pressure being a function of the angular distance of the line from the center line of the wing. The pressure is noted to be constant over the elementary triangular area indicated in figure 6. If now the differential hinge moment caused by this pressure acting over the flap can be determined, the resulting expression can be integrated to give the entire hinge moment of the flap.

For the present, the net pressure over the top and bottom surfaces can be written as P. If the part of the incremental area contained between the flap hinge line and the wing trailing edge is called A, if the remainder of the incremental area is called B, and further if r is used to denote the distance of the centroid of an area from an axis, with subscripts to denote the axis and the area (see fig. 6 for axes used), an expression for the differential hinge moment of the flap can be written as

$$dH = PAr_{HL_A} = P\left[(A + B)r_{o_{A+B}} - Br_{o_B} - (A + B - B)R\right] \qquad (24)$$

The various areas and centroids can be written as follows (see fig. 6):

$$A + B = \frac{c}{2}\,db_f$$

$$B = \frac{R}{2}\,db_f'$$

$$A + B - B = \frac{c}{2}\,db_f - \frac{R}{2}\,db_f'$$

$$r_{o_B} = \frac{2}{3}R$$

The following equations can also be written

$$r_{o_{A+B}} = \frac{2}{3}c(\sin\epsilon + \cos\epsilon\tan\zeta)$$

$$R = 2\left(c - c_f\right)\sin\epsilon$$

Expression of equation (24) in terms of t is convenient where

$$t \equiv \frac{\tan\zeta}{\tan\epsilon} \qquad (25)$$

If a number n is defined as

$$n \equiv \frac{\tan \mu}{\tan \epsilon} \qquad (26)$$

$t = 0$ on the wing center line, $t = n$ on the Mach line, and $t = 1$ on the wing leading edge. The numbers t and n have here the same significance as in reference 2. The intersection of the hinge line with the wing trailing edge corresponds to $t = 1 - 2\left(\frac{c_f}{c}\right)$. This value of t is called t_o. In order to express equation (24) in terms of t, the following equations can be written

$$db_f = c \tan \epsilon \, dt$$

and

$$db_f' = 2(c - c_f) \sec \epsilon \frac{dt}{(t + 1)^2}$$

By substitution in equation (24) and simplification, the result obtained is

$$dH = \frac{\sin^2 \epsilon}{\cos \epsilon} \left\{ \left[\frac{c^3}{3} - c^2\left(c - c_f\right) \right] P \, dt + \frac{c^3}{3} Pt \, dt + \frac{4}{3}\left(c - c_f\right)^3 \frac{P \, dt}{(t + 1)^2} \right\}$$

where P is a function of t. For convenience in notation, the chord functions are given special names:

$$F_1 \equiv \frac{c^3}{3} - c^2\left(c - c_f\right)$$

$$F_2 \equiv \frac{c^3}{3}$$

$$F_3 \equiv \frac{4}{3}\left(c - c_f\right)^3$$

The expression for dH then becomes

$$dH = \frac{\sin^2\epsilon}{\cos\epsilon}\left[F_1 P\,dt + F_2 Pt\,dt + F_3\frac{P\,dt}{(t+1)^2}\right] \tag{27}$$

An expression for P can be obtained from equations (9), (34), and (35) of reference 2. Equation (9) of reference 2, in the notation of the present paper, defines a pressure coefficient as

$$C_p = \frac{p - p_o}{\rho V^2/2} = -\frac{2\phi_x}{V} \tag{28}$$

where

p pressure acting on one surface of wing

ϕ_x disturbance velocity in x-direction

If, as before, P is the pressure difference between upper and lower surfaces, then

$$P = 2\rho V\phi_x \tag{29}$$

For the part of the wing ahead of the Mach line $(t > n)$, ϕ_x is given by equation (34) of reference 2 as

$$\phi_{x_1} = -\frac{w}{\beta\sqrt{1 - n^2}}$$

where w, the vertical disturbance velocity, is αV in the present case.

Behind the Mach line $(t < n)$, equation (35) of reference 2 gives

$$\phi_{x_2} = -\frac{w}{\beta\sqrt{1 - n^2}} + \frac{w}{\beta\sqrt{1 - n^2}}\left(\frac{2}{\pi}\sin^{-1}\sqrt{\frac{n^2 - t^2}{1 - t^2}}\right)$$

(The subscripts are added for convenience.) When it is remembered that these different expressions for the potential are necessary ahead of and behind the Mach line, equation (27) can be integrated to give the total hinge moment of the flap:

$$H = 2\rho V \frac{\sin^2\epsilon}{\cos\epsilon}\left\{F_1\left(\int_n^1 \phi_{x_1}\,dt + \int_{t_o}^n \phi_{x_2}\,dt\right)\right.$$

$$+ F_2\left(\int_n^1 \phi_{x_1} t\,dt + \int_{t_o}^n \phi_{x_2} t\,dt\right)$$

$$\left. + F_3\left[\int_n^1 \frac{\phi_{x_1}\,dt}{(t+1)^2} + \int_{t_o}^n \frac{\phi_{x_2}\,dt}{(t+1)^2}\right]\right\}$$

Upon substituting the values of ϕ_{x_1} and ϕ_{x_2}, this equation becomes

$$H = -\frac{2\rho\alpha V^2}{\beta\sqrt{1 - n^2}}\frac{\sin^2\epsilon}{\cos\epsilon}\left[F_1\int_{t_o}^1 dt + F_2\int_{t_o}^1 t\,dt + F_3\int_{t_o}^1 \frac{dt}{(t+1)^2}\right]$$

$$+ \frac{4\rho\alpha V^2}{\pi\beta\sqrt{1 - n^2}}\frac{\sin^2\epsilon}{\cos\epsilon}\left[F_1\int_{t_o}^n \sin^{-1}\sigma\,dt + F_2\int_{t_o}^n t\sin^{-1}\sigma\,dt\right.$$

$$\left. + F_3\int_{t_o}^n \frac{\sin^{-1}\sigma\,dt}{(t+1)^2}\right] \qquad (30)$$

where

$$\sigma = \sqrt{\frac{n^2 - t^2}{1 - t^2}}$$

Forming the hinge-moment coefficient per unit angle of attack gives

$$C_{h_\alpha} = \frac{\partial H/\partial \alpha}{q b_f' \bar{c}_f^2}$$

where b_f' and $\bar{c}_f^2$ are given by equations (19) and (20). Performing the indicated operation, simplifying, and expressing the result as $C_{h_\alpha}\beta/2$ give

$$\frac{C_{h_\alpha}\beta}{2} = -\frac{3}{2\sqrt{1 - n^2}}\left[G_1 \int_{t_o}^{1} dt + G_2 \int_{t_o}^{1} t\, dt + G_3 \int_{t_o}^{1} \frac{dt}{(t + 1)^2}\right]$$

$$+ \frac{3}{\pi\sqrt{1 - n^2}}\left[G_1 \int_{t_o}^{n} \sin^{-1}\sigma\, dt + G_2 \int_{t_o}^{n} t \sin^{-1}\sigma\, dt\right.$$

$$\left. + G_3 \int_{t_o}^{n} \frac{\sin^{-1}\sigma\, dt}{(t + 1)^2}\right] \qquad (31)$$

where

$$G_1 \equiv \frac{F_1}{c_f^3} = -\frac{2}{3}\left(\frac{c}{c_f}\right)^3 + \left(\frac{c}{c_f}\right)^2$$

$$G_2 \equiv \frac{F_2}{c_f^3} = \frac{1}{3}\left(\frac{c}{c_f}\right)^3$$

$$G_3 \equiv \frac{F_3}{c_f^3} = \frac{4}{3}\left(\frac{c}{c_f} - 1\right)^3$$

The quantity in the first bracket of equation (31), which arose from integrating a constant pressure over the flap, has the constant value 2/3, so that equation (31) may be simplified to read

$$\frac{C_{h_\alpha}\beta}{2} = -\frac{1}{\sqrt{1 - n^2}} + \frac{3}{\pi\sqrt{1 - n^2}}\left[G_1 \int_{t_o}^{n} \sin^{-1}\sigma \, dt + G_2 \int_{t_o}^{n} t \sin^{-1}\sigma \, dt + G_3 \int_{t_o}^{n} \frac{\sin^{-1}\sigma \, dt}{(t + 1)^2}\right] \tag{32}$$

This is the expression for the general case in which the Mach line from the wing apex intersects the flap. For the case in which the Mach line does not intersect the flap, $C_{h_\alpha}\beta/2$ is simply the first term of equation (32). This fact is easily seen physically by recalling that everywhere outside the Mach line the pressure is a constant dependent only on n. Therefore, if for a given value of n various sizes of flaps all lying outside the Mach line are considered, all these flaps will have the same value for C_{h_α}. This reasoning can be extended further. Consider the flap size to be increased so that part of the flap now lies inside the Mach line. This part of the flap is acted on by a lower pressure than the part outside the Mach line, so that the value of C_{h_α} would be expected to be lower than that for a flap lying wholly outside the Mach line. A pictorial representation of the pressure distribution on the wing is given in figure 7.

The integrals occurring in equation (32) are evaluated in the appendix. Values of $-C_{h_\alpha}\beta/2$ have been calculated and are presented in figure 8. The value of C_{h_α} for the two-dimensional case (see reference 6) is

$$C_{h_{\alpha_\infty}} = -\frac{2}{\beta}$$

or

$$-\frac{C_{h_{\alpha_\infty}}\beta}{2} = 1 \tag{33}$$

therefore, figure 8 also represents the ratio of C_{h_α} for the triangular case to C_{h_α} for the two-dimensional case. In all cases the value of C_{h_α} for the present configuration is greater than the corresponding two-dimensional value. As is to be expected from the qualitative reasoning given before, C_{h_α} decreases as the flap chord increases and as the Mach line moves farther behind the leading edge. (The decrease with increasing flap chord does not occur, of course, when the flap is wholly outside the Mach line.)

DISCUSSION AND CONCLUDING REMARKS

The efficiency of a control surface may be indicated by the ratio of α_δ to C_{h_δ}. In effect, this ratio represents the lift produced upon application of a given control force; therefore, the larger the ratio, the more efficient the control surface. The value of the ratio $\alpha_\delta/C_{h_\delta}$ for the configuration investigated in the present paper to the corresponding ratio for the two-dimensional case may be found by using equations (4), (7), and (23); the result is

$$\frac{\alpha_\delta/C_{h_\delta}}{\alpha_{\delta_\infty}/C_{h_{\delta_\infty}}} = \frac{2(c_f/c)^2}{(c_f/c)_\infty} = \frac{S_f/S}{(S_f/S)_\infty}$$

which shows that for the same ratio of flap area to wing area the efficiency of the triangular control surface on the triangular wing is equal to that of the two-dimensional wing-flap combination.

A similar comparison can be made of the rate of roll for a given control force. By using equations (17), (18), and (23), the following equation is obtained

$$\frac{\dfrac{pb/2V}{\delta}}{\dfrac{C_{h_\delta}}{\left(\dfrac{pb/2V}{\delta}\right)_\infty}} = 4\left(1 - \frac{c_f}{c}\right)\frac{2\left(c_f/c\right)^2}{\left(c_f/c\right)_\infty} = 4\left(1 - \frac{c_f}{c}\right)\frac{S_f/S}{\left(S_f/S\right)_\infty}$$

For equal flap area ratios and $\frac{c_f}{c} = \frac{1}{2}$, the rate of roll per unit hinge-moment coefficient is twice as large for the triangular case as for the two-dimensional case. This difference is a direct result of the difference in damping coefficient for the two cases (see equations (15) and (16)); for equal flap area ratios the quantity $\dfrac{C_{l_\delta}/C_{h_\delta}}{\left(C_{l_\delta}/C_{h_\delta}\right)_\infty}$ is unity. In these comparisons the effect on the hinge moment of the asymmetrical angle-of-attack distribution when the wing is rolling has been neglected.

The values of C_{h_α} are high compared either with C_{h_δ} or with the two-dimensional values of C_{h_α}. An appreciable balancing effect is thus indicated for cases in which an angle-of-attack response to control-surface deflection is allowed. If the present arrangement were used as a horizontal tail, the effect on the stick-free longitudinal stability would have to be considered. In reference 8 the ratio of tail lift-curve slope with controls free to that with controls fixed is shown to be

$$\frac{C_{L_{\alpha_{free}}}}{C_{L_{\alpha_{fixed}}}} = 1 - \frac{C_{L_\delta}}{C_{L_\alpha}}\frac{C_{h_\alpha}}{C_{h_\delta}}$$

which becomes for the present case

$$\frac{C_{L_{\alpha_{free}}}}{C_{L_{\alpha_{fixed}}}} = 1 - \frac{S_f}{S}\left|C_{h_\alpha}\frac{\beta}{2}\right|$$

This ratio is a measure of the destabilizing effect caused by freeing the controls and may be used as indicated in reference 8 to estimate the resulting shift in neutral point.

Langley Memorial Aeronautical Laboratory
National Advisory Committee for Aeronautics
Langley Field, Va., March 23, 1948

APPENDIX

INTEGRATIONS FOR HINGE MOMENT DUE TO ANGLE OF ATTACK

Equation (32) contains three integrals, the first of which is

$$\int_{t_o}^{n} \sin^{-1}\sigma \, dt \tag{A1}$$

where

$$\sigma = \sqrt{\frac{n^2 - t^2}{1 - t^2}}$$

This expression may be integrated by parts to give

$$\int \sin^{-1}\sigma \, dt = t \sin^{-1}\sigma + \left(1 - n^2\right)^{1/2} \int \frac{t^2 \, dt}{\left(1 - t^2\right)\left(n^2 - t^2\right)^{1/2}} \tag{A2}$$

The integral in equation (A2) can be evaluated by making the substitution $t = n \sin\theta$. The integral then becomes

$$\int \frac{t^2 \, dt}{\left(1 - t^2\right)\left(n^2 - t^2\right)^{1/2}} = \int \frac{n^2 \sin^2\theta \, d\theta}{1 - n^2 \sin^2\theta} \tag{A3}$$

This integral can be simplified by division and by separation into partial fractions which gives

$$\int \frac{n^2 \sin^2\theta \, d\theta}{-n^2 \sin^2\theta + 1} = -\int d\theta + \frac{1}{2} \int \frac{d\theta}{1 + n \sin\theta} + \frac{1}{2} \int \frac{d\theta}{1 - n \sin\theta} \tag{A4}$$

The first integral on the right-hand side of equation (A4) is simply

$$-\int d\theta = -\sin^{-1}\frac{t}{n} \tag{A5}$$

The second and third integrals can be evaluated (reference 9, equation (298)) to give

$$\left.\begin{aligned}\int \frac{d\theta}{1 + n\sin\theta} &= \frac{2}{\sqrt{1 - n^2}}\tan^{-1}\left(\frac{n - \sqrt{n^2 - t^2}}{t\sqrt{1 - n^2}} + \frac{n}{\sqrt{1 - n^2}}\right)\\ \int \frac{dt}{1 - n\sin\theta} &= \frac{2}{\sqrt{1 - n^2}}\tan^{-1}\left(\frac{n - \sqrt{n^2 - t^2}}{t\sqrt{1 - n^2}} - \frac{n}{\sqrt{1 - n^2}}\right)\end{aligned}\right\} \tag{A6}$$

Expression (A1) then becomes

$$\begin{aligned}\int_{t_o}^{n} \sin^{-1}\sqrt{\frac{n^2 - t^2}{1 - t^2}}\,dt = \Bigg[&t\sin^{-1}\sqrt{\frac{n^2 - t^2}{1 - t^2}} - \left(1 - n^2\right)^{1/2}\sin^{-1}\frac{t}{n}\\ &+ \tan^{-1}\left(\frac{n - \sqrt{n^2 - t^2}}{t\sqrt{1 - n^2}} + \frac{n}{\sqrt{1 - n^2}}\right)\\ &+ \tan^{-1}\left(\frac{n - \sqrt{n^2 - t^2}}{t\sqrt{1 - n^2}} - \frac{n}{\sqrt{1 - n^2}}\right)\Bigg]_{t_o}^{n}\end{aligned} \tag{A7}$$

The second integral occurring in equation (32) is

$$\int_{t_o}^{n} t\sin^{-1}\sigma\,dt \tag{A8}$$

where again

$$\sigma = \sqrt{\frac{n^2 - t^2}{1 - t^2}}$$

This equation can be integrated in much the same manner as the first integral. First, an integration by parts gives

$$\int t \sin^{-1}\sigma \, dt = \frac{t^2}{2} \sin^{-1}\sigma + \frac{(1 - n^2)^{1/2}}{2} \int \frac{t^3 \, dt}{(1 - t^2)(n^2 - t^2)^{1/2}} \quad \text{(A9)}$$

The integral in equation (A9) can be evaluated by making the substitution $t = n \sin\theta$ which gives

$$\int \frac{t^3 \, dt}{(1 - t^2)(n^2 - t^2)^{1/2}} = \int \frac{n^3 \sin^3\theta \, d\theta}{1 - n^2 \sin^2\theta} \quad \text{(A10)}$$

As before, division and separation into partial fractions give

$$\int \frac{n^3 \sin^3\theta \, d\theta}{1 - n^2 \sin^2\theta} = -\int n \sin\theta \, d\theta - \frac{1}{2}\int \frac{d\theta}{1 + n \sin\theta} + \frac{1}{2}\int \frac{d\theta}{1 - n \sin\theta} \quad \text{(A11)}$$

The second two integrals on the right-hand side of equation (A11) have already been evaluated (equation (A6)). The first integral is

$$-\int n \sin\theta \, d\theta = n \cos\theta = \sqrt{n^2 - t^2} \quad \text{(A12)}$$

Equation (A8) then becomes

$$\int_{t_o}^{n} t \sin^{-1}\sqrt{\frac{n^2 - t^2}{1 - t^2}}\, dt = \left[\frac{t^2}{2}\sin^{-1}\sqrt{\frac{n^2 - t^2}{1 - t^2}}\right.$$

$$+ \frac{(1 - n^2)^{1/2}(n^2 - t^2)^{1/2}}{2}$$

$$- \frac{1}{2}\tan^{-1}\left(\frac{n - \sqrt{n^2 - t^2}}{t\sqrt{1 - n^2}} + \frac{n}{\sqrt{1 - n^2}}\right)$$

$$\left. + \frac{1}{2}\tan^{-1}\left(\frac{n - \sqrt{n^2 - t^2}}{t\sqrt{1 - n^2}} - \frac{n}{\sqrt{1 - n^2}}\right)\right]_{t_o}^{n} \qquad (A13)$$

The last integral to be evaluated is

$$\int_{t_o}^{n} \frac{\sin^{-1}\sigma\, dt}{(t + 1)^2} \qquad (A14)$$

The same general procedure used for the previous two integrals can be employed. The first integration by parts gives

$$\int \frac{\sin^{-1}\sigma\, dt}{(t + 1)^2} = -\frac{\sin^{-1}\sigma}{t + 1} - (1 - n^2)^{1/2}\int \frac{t\, dt}{(1 + t)(1 - t^2)(n^2 - t^2)^{1/2}} \qquad (A15)$$

Substitution of $t = n \sin\theta$ gives

$$\int \frac{t\,dt}{(1+t)(1-t^2)(n^2-t^2)^{1/2}} = \int \frac{n \sin\theta\,d\theta}{(1+n\sin\theta)^2(1-n\sin\theta)} \tag{A16}$$

Separating into partial fractions gives

$$\int \frac{n \sin\theta\,d\theta}{(1+n\sin\theta)^2(1-n\sin\theta)} = -\frac{1}{2}\int \frac{d\theta}{(1+n\sin\theta)^2}$$

$$+\frac{1}{4}\int \frac{d\theta}{1+n\sin\theta} + \frac{1}{4}\int \frac{d\theta}{1-n\sin\theta} \tag{A17}$$

The last two integrals have been evaluated (equation (A6)). With the aid of reference 9, equations (318), (308), and (300), the first integral can be evaluated to give

$$\int \frac{d\theta}{(1+n\sin\theta)^2} = \frac{1}{1-n^2}\left[\frac{\sqrt{n^2-t^2}}{1+t} - \frac{2}{\sqrt{1-n^2}}\tan^{-1}\sqrt{\frac{(1-n)(n-t)}{(1+n)(n+t)}}\right] \tag{A18}$$

Expression (A14) then becomes

$$\int_{t_o}^{n} \frac{1}{(t+1)^2} \sin^{-1}\sqrt{\frac{n^2-t^2}{1-t^2}}\,dt = \left[-\frac{\sin^{-1}\sqrt{\frac{n^2-t^2}{1-t^2}}}{1+t} \right.$$

$$+ \frac{1}{2\sqrt{1-n^2}}\left[\frac{\sqrt{n^2-t^2}}{1+t} - \frac{2}{\sqrt{1-n^2}} \tan^{-1}\sqrt{\frac{(1-n)(n-t)}{(1+n)(n+t)}}\right]$$

$$- \frac{1}{2}\tan^{-1}\left(\frac{n-\sqrt{n^2-t^2}}{t\sqrt{1-n^2}} + \frac{n}{\sqrt{1-n^2}}\right)$$

$$\left. - \frac{1}{2}\tan^{-1}\left(\frac{n-\sqrt{n^2-t^2}}{t\sqrt{1-n^2}} - \frac{n}{\sqrt{1-n^2}}\right)\right]_{t_o}^{n} \qquad \text{(A19)}$$

REFERENCES

1. Jones, Robert T.: Properties of Low-Aspect-Ratio Pointed Wings at Speeds below and above the Speed of Sound. NACA TN No. 1032, 1946.

2. Puckett, Allen E.: Supersonic Wave Drag of Thin Airfoils. Jour. Aero. Sci., vol. 13, no. 9, Sept. 1946, pp. 475-484.

3. Brown, Clinton E.: Theoretical Lift and Drag of Thin Triangular Wings at Supersonic Speeds. NACA TN No. 1183, 1946.

4. Stewart, H. J.: The Lift of a Delta Wing at Supersonic Speeds. Quarterly Appl. Math., vol. IV, no. 3, Oct. 1946, pp. 246-254.

5. Ribner, Herbert S.: The Stability Derivatives of Low-Aspect-Ratio Triangular Wings at Subsonic and Supersonic Speeds. NACA TN No. 1423, 1947.

6. Collar, A. R.: Theoretical Forces and Moments on a Thin Aerofoil with Hinged Flap at Supersonic Speeds. R. & M. No. 2004, British A.R.C., 1943.

7. Brown, Clinton E., and Adams, Mac C.: Damping in Pitch and Roll of Triangular Wings at Supersonic Speeds. NACA TN No. 1566, 1948.

8. Schuldenfrei, Marvin: Some Notes on the Determination of the Stick-Free Neutral Point from Wind-Tunnel Data. NACA RB No. 4B21, 1944.

9. Peirce, B. O.: A Short Table of Integrals. Second ed., Ginn and Co., 1910.

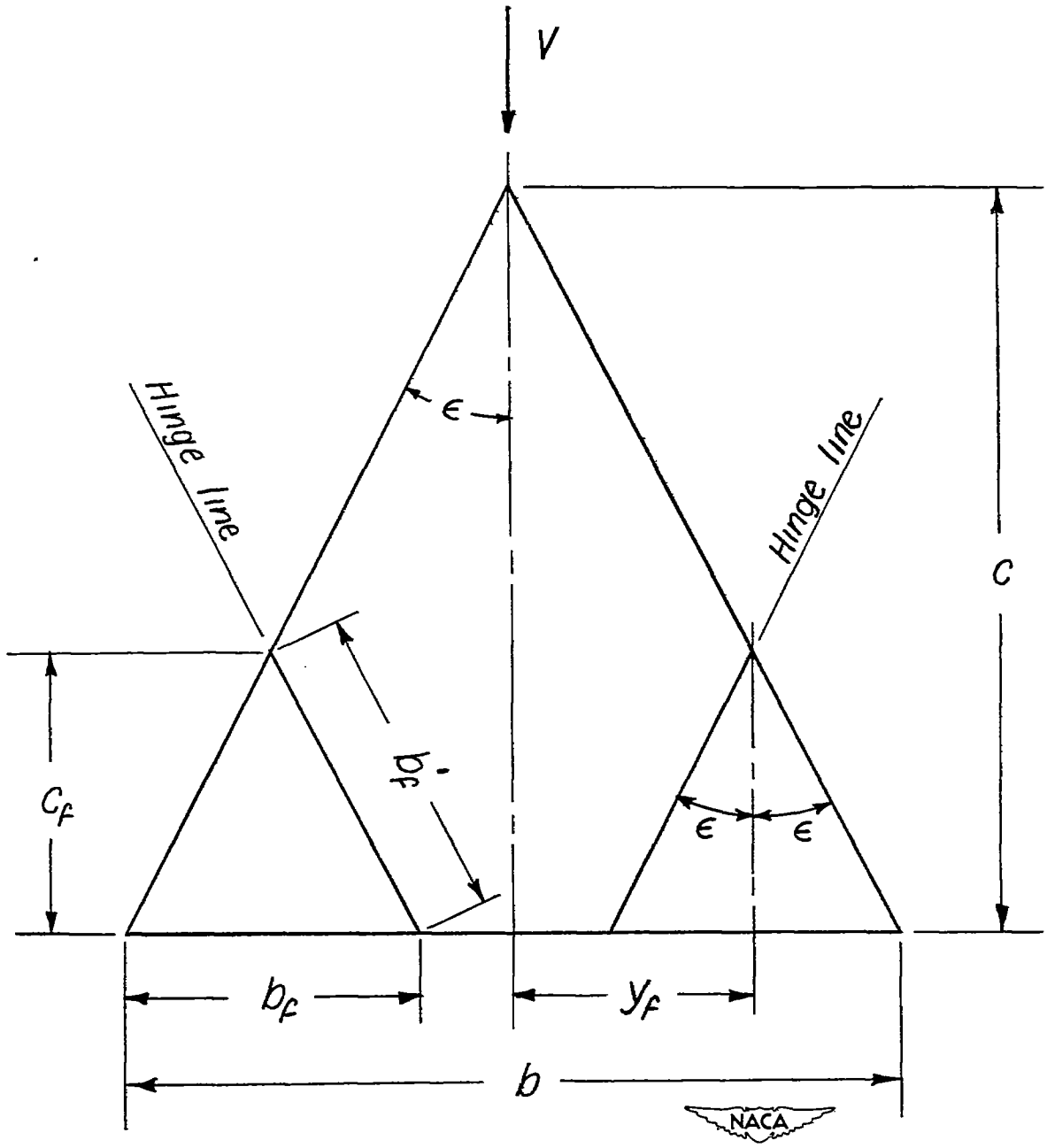

Figure 1.- Control-surface configuration.

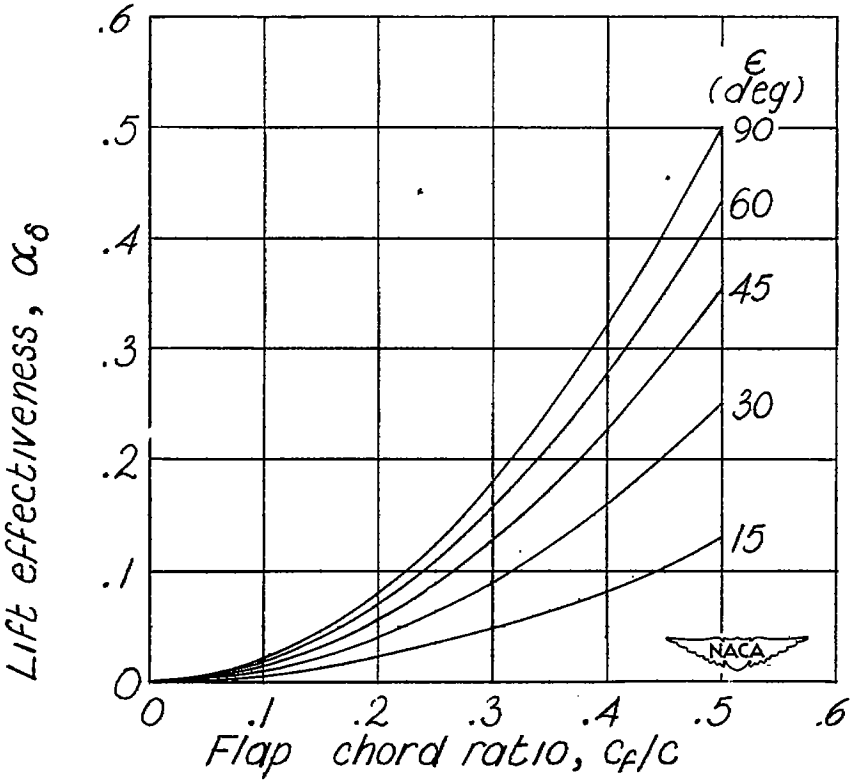

Figure 2.- Lift effectiveness of triangular-tip control surfaces on triangular wings.

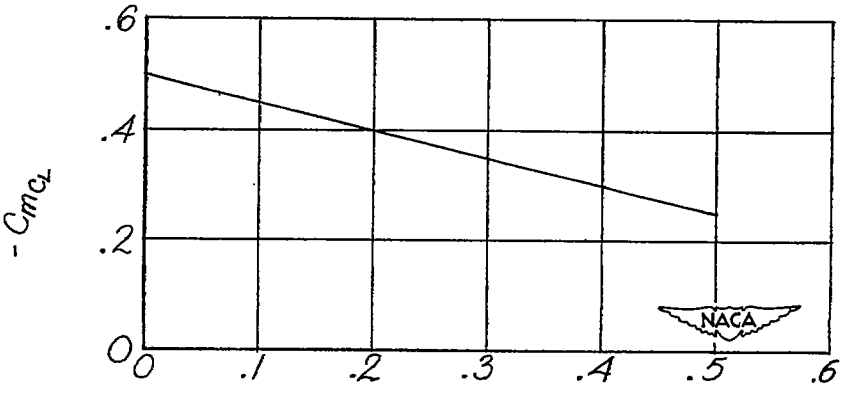

Figure 3.- Pitching-moment characteristics of triangular-tip control surfaces on triangular wings.

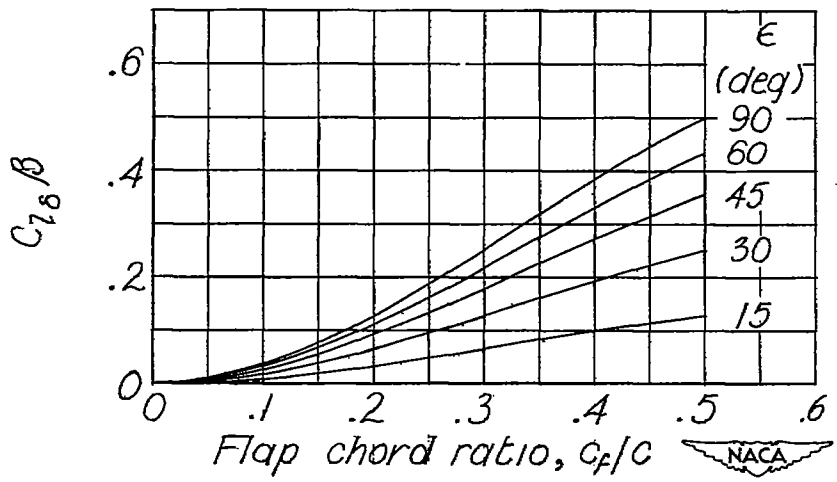

Figure 4.- Rolling-moment effectiveness of triangular-tip control surfaces on triangular wings.

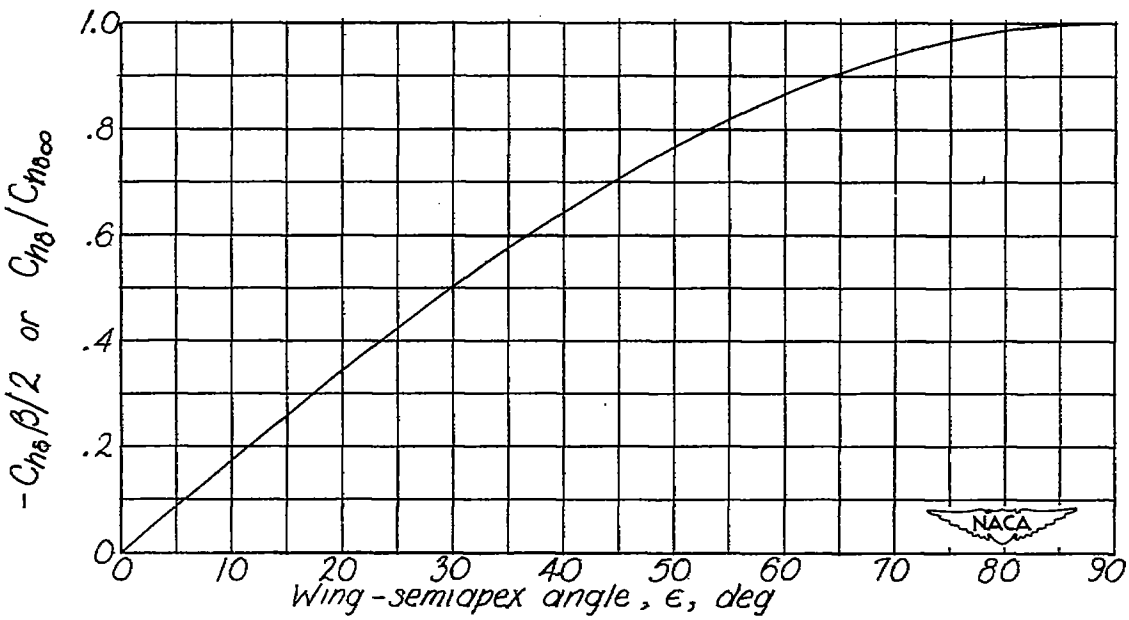

Figure 5.- Characteristics of hinge moment due to control deflection. Triangular-tip control surfaces on triangular wings.

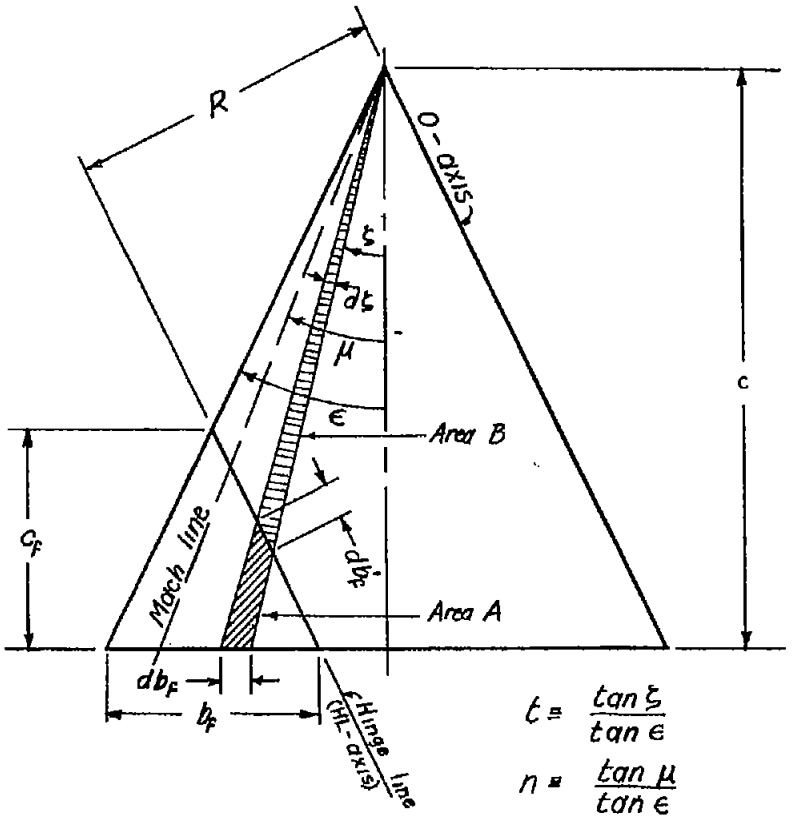

Figure 6.- Notation for derivation of hinge moment due to angle of attack.

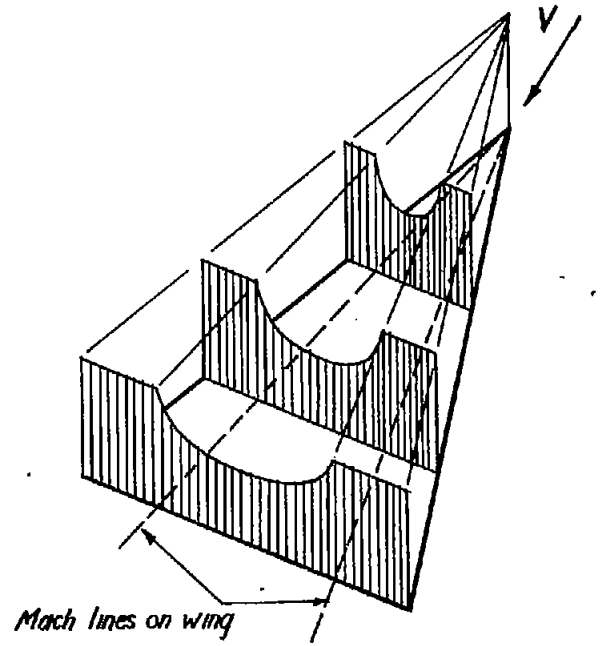

Figure 7.- Type of pressure distribution on the wing at an angle of attack.

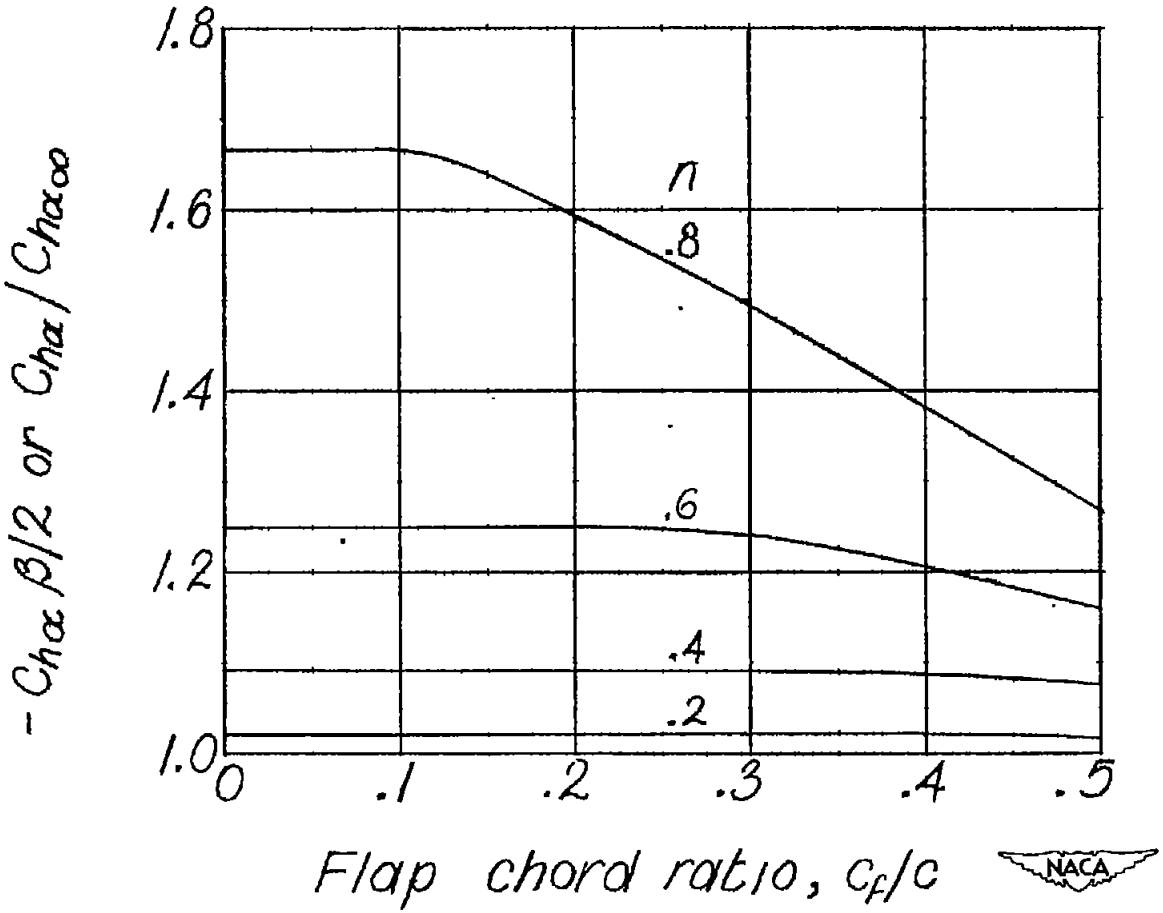

Figure 8.- Characteristics of hinge moment due to angle of attack. Triangular-tip control surfaces on triangular wings.